

Bull. Pure Appl. Sci. Sect. E Math. Stat. **39E**(1), 84–97 (2020) e-ISSN:2320-3226, Print ISSN:0970-6577 DOI: 10.5958/2320-3226.2020.00007.7 ©Dr. A.K. Sharma, BPAS PUBLICATIONS,

387-RPS- DDA Flat, Mansarover Park, Shahdara, Delhi-110032, India. 2020

Bulletin of Pure and Applied Sciences Section - E - Mathematics & Statistics

Website: https://www.bpasjournals.com/

Heat transfer on unsteady MHD convective flow of nanofluids in a rotating frame *

B. Veera Sankar 1,† and B. Rama Bhupal Reddv 2

- Research Scholar, Department of Mathematics, Rayalaseema University, Kurnool, Andhra Pradesh-518007, India.
 - 2. Department of Mathematics, KSRM College of Engineering, Kadapa, Andhra Pradesh-516003, India.
 - 1. E-mail: veerasankar4@gmail.com , 2. E-mail: reddybrb@gmail.com

Abstract In this paper, the unsteady MHD free convective rotating flow of nanofluids (Cu–water and Al_2O_3 –water) in a porous medium bounded by a moving vertical semi-infinite permeable flat plate with constant heat source and convective boundary condition is studied. The slip velocity is assumed to oscillate in time with constant frequency so that the solutions of the boundary layer are the same oscillatory type. The equations for the governing flow are solved analytically by perturbation approximation. The effects of various parameters on the flow are discussed through graphs and tables.

Key words Heat transfer, Porous medium Nanofluids, Rotating frame, Convective flow.

2020 Mathematics Subject Classification 76R99, 76S05, 76S99, 76W05, 76W99.

Nomenclature of symbols

u, v, w, velocity components along x, y and z-axes respectively;

 $\beta_{n,f}$, coefficient of the thermal expansion of nanofluid;

 K_{nf} , thermal conductivity of nanofluid;

 U_r , the uniform reference velocity;

- ε , the small constant quantity;
- σ , electric conductivity of the fluid;

 ρ_{nf} , density of the nanofluid;

 μ_{nf} , viscosity of the nanofluid;

 $(\rho C_p)_{nf}$, heat capacitance of the nanofluid;

g, acceleration due to gravity;

- k, permeability of porous medium;
- T, temperature of the nanofluid;
- Q, temperature dependent volumetric rate of heat source;

 α_{nf} , thermal diffusivity of the nanofluid;

 $(\rho\beta)_{nf}$, the thermal expansion coefficient of the nanofluid;

^{*} Communicated, edited and typeset in Latex by Lalit Mohan Upadhyaya (Editor-in-Chief). Received December 26, 2018 / Revised August 03, 2019 / Accepted August 31, 2019. Online First Published on June 30, 2020 at https://www.bpasjournals.com/.

[†]Corresponding author B. Veera Sankar, E-mail: veerasankar4@gmail.com

 ϕ , solid volume fraction of the nanoparticles;

 w_0 , the normal velocity at the plate;

 ν_f , kinematic viscosity of nanofluid;

R, rotational parameter;

M, magnetic field parameter,;

Pr, Prandtl number;

 Ω , Angular velocity;

 γ , convective parameter;

 Re_x ,Local Reynolds number;

 τ , skin friction parameter;

Nu, Nusselt number;

n, frequency of oscillation;

t, time.

Nomenclature of Subscripts

f, base fluid; nf, nano-fluid;

s, nanosolid paricles.

1 Introduction

Major interest in the study of convective heat transfer of nanofluids in sciences and engineering is very important on account of its various applications. Water, ethylene glycol and engine oil are heating or cooling agents and play a decisive job in thermal management of many industries with poor thermal conductivity. We enhance thermal conductivity for extended surfaces, mini-channels and micro-channels. Concrete materials have higher thermal conductivities.

The word nanofluid was introduced first by Choi [1]. Nano-particles are a viaduct between immensity materials and atomic or molecular compositions. Some of the nano-particles used for fluid mechanical models are Al, Cu, Fe and Ti or their oxides. Some studies [2, 3, 4, 5] illustrate the small volumetric fraction of nano-particles. The thermal conductivity of nanofluid is enhanced together with the thermal conductivity of the base fluid and instability induced by their action donates an amazing perfection to the coefficient of convective heat transfer. Advanced nuclear system [6] has good application use of nanofluids. Micro-channel cooling and miniaturization of the system, heat transfer system size reduction, improved heat transfer and minimal clogging are the advantages of nanofluids. Convective flow of nanofluids past porous media is broadly investigated due to its wide applications in engineering [7,8,9,10,11,12]. Gilles et al. [13], Jou and Tzeng [14], Ho et al. [15,16], Congedo et al. [17] and Ghasemi and Aminossadati [18] discussed natural convection heat transfer in nanofluids. The two dimensional natural convection flow of a nanofluid in an enclosure was discussed by Khanafer et al. [19]. A new friction factor to portray the upshot of nanoparticles on the convective instability has been introduced by Kim et al. [20]. MHD rotating flows of non-Newtonian fluids have many applications in turbo machinery, geophysics, meteorology and some other fields. Bakr [21] and Das [22] discussed free convection flow of micropolar fluid in a rotating channel. Recently, Hamad and Pop [24] investigated free convective MHD rotating flow in a nanofluid with constant heat source and a new nanofluid model was also proposed by Tiwari and Das [23]. The heat transfer problems for boundary layer flow concerning a convective boundary condition were discussed by Aziz [25], Makinde and Aziz [26], Ishak [27] and Yacob et al. [28]. Veera Krishna and Chamkha [34] investigated the diffusion-thermo, radiation-absorption and Hall and ion slip effects on MHD free convective rotating flow of nano-fluids (Ag and TiO₂) past a semi-infinite permeable moving plate with constant heat source. In another recent paper Veera Krishna and Chamkha [35] discussed the MHD squeezing flow of a water-based nanofluid through a saturated porous medium between two parallel disks, taking the Hall current into account. Hall and ion slip effects on unsteady MHD convective rotating flow of nanofluids are discussed by Veera Krishna and Chamkha in [36].

But, so far, no attempt is made to apply the convective surface boundary condition to analyze the boundary layer rotating flow of a nanofluid past a porous vertical moving plate. Keeping the above mentioned facts in mind, the unsteady MHD free convective rotating flow of nanofluids (Cu–water and Al_2O_3 —water) in a porous medium bounded by a moving vertical semi-infinite permeable flat plate with constant heat source and convective boundary condition is studied theoretically in this paper.



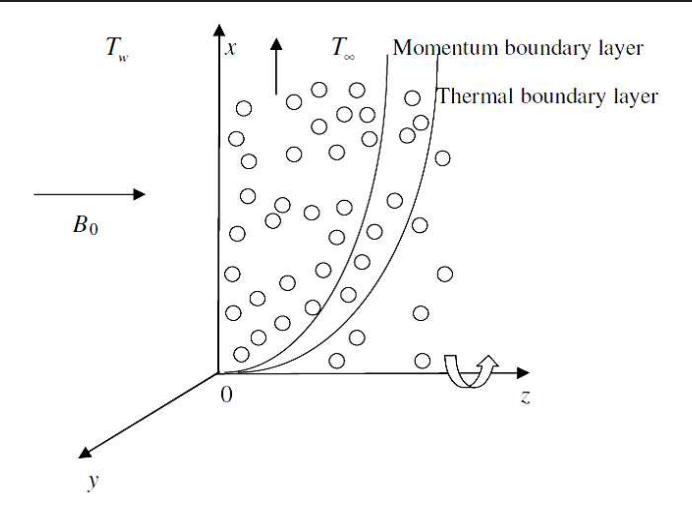


Fig. 1: Physical configuration of the problem.

2 Formulation and solution of the problem

We consider the unsteady free convective flow of nanofluids (Cu and Al₂O₃) of ambient temperature T_{∞} over a vertical semi-infinite moving permeable plate entrenched in a homogeneous porous medium under the thermal buoyancy effect with stable heat source and convective boundary condition. We assume a uniform shaped and sized nanoparticles. Also both the fluid phase and nanoparticles are in thermal equilibrium state. Fig. 1 portrays the physical model of the problem. The flow is assumed to be in the x-direction which is obtained along the plate in the ascending direction and the z-axis is taken normal to it. The entire system is rotating with an angular velocity Ω about the z-axis. An unvarying peripheral magnetic field B_0 is taken to be acting along the z-axis. Also there is no applied voltage (i.e., E=0). The induced magnetic field is tiny compared to the external magnetic field. Hence, a small magnetic Reynolds number for the oscillating plate (see Liron and Wilhelm [29]). Due to the semi-infinite plate surface assumption, all the variables are functions of z and time t only.

Under the boundary layer approximations, the basic equations that describe the physical situation are given by

$$\frac{\partial w}{\partial z} = 0$$

$$\frac{\partial u}{\partial t} + w \frac{\partial u}{\partial z} - 2\Omega v = \frac{1}{\rho_{nf}} \left[\mu_{nf} \frac{\partial^2 u}{\partial z^2} + (\rho \beta)_{nf} g (T - T_{\infty}) - \frac{\mu_{nf} u}{k} - \sigma B_0^2 u \right]$$
(2.1)

$$\frac{\partial v}{\partial t} + w \frac{\partial v}{\partial z} + 2\Omega u = \frac{1}{\rho_{nf}} \left[\mu_{nf} \frac{\partial^2 v}{\partial z^2} - \frac{\mu_{nf} v}{k} - \sigma B_0^2 v \right]$$
 (2.3)

$$\frac{\partial T}{\partial t} + w \frac{\partial T}{\partial z} = \alpha_{nf} \frac{\partial^2 T}{\partial z^2} - \frac{Q}{(\rho C_p)_{nf}} (T - T_\infty)$$
(2.4)

The boundary conditions are given by

$$u = v = 0, T = T_{\infty} \text{ for } t \le 0$$
 (2.5)

(2.1)

$$u = U_r \left[1 + \frac{\varepsilon}{2} \left\{ \exp\left(int\right) + \exp\left(-int\right) \right\} \right], v = 0, -K_{nf} \frac{\partial T}{\partial z} = h_f \left(T_w - T_\infty \right) \text{ at } z = 0 \\ u \to 0, \ v \to 0, \ T \to T_\infty \text{ as } z \to \infty$$
 (2.6)

The oscillatory plate velocity is assumed in (2.6) (see, Ganapathy [30]). The effective density of the nanofluid is given by

$$\rho_{nf} = (1 - \phi) \rho_f + \phi \rho_s. \tag{2.7}$$

The thermal diffusivity of the nanofluid is

$$\alpha_{nf} = \frac{K_{nf}}{\left(\rho C_p\right)_{nf}},\tag{2.8}$$



where, the heat capacitance C_p of the nanofluid is

$$(\rho C_p)_{nf} = (1 - \phi) (\rho C_p)_f + \phi (\rho C_p)_s.$$
(2.9)

The thermal conductivity of the nanofluid k_{nf} for spherical nanoparticles is as given in Maxwell [31]

$$\frac{k_{nf}}{k_f} = \frac{(k_s + 2k_f) - 2\phi \ (k_f - k_s)}{(k_s + 2k_f) + 2\phi \ (k_f - k_s)}.$$
 (2.10)

The thermal expansion coefficient of the nanofluid is

$$(\rho \beta)_{nf} = (1 - \phi) (\rho \beta)_f + \phi (\rho \beta)_s. \tag{2.11}$$

Finally the effective dynamic viscosity of the nanofluid given by Brinkman [32] as

$$\mu_{nf} = \frac{\mu_f}{(1-\phi)^{2.5}}. (2.12)$$

The thermo-physical properties of the nanofluids are given in Oztop and Abu-Nada [33, Table 1].

$$w = -w_0 \tag{2.13}$$

where, the w_0 represents the normal velocity at the plate which is positive for suction and negative for injection.

Let us introduce the following dimensionless variables:

$$u' = \frac{u}{U_r}, v' = \frac{v}{U_r}, z' = \frac{zU_r}{v_f}, t' = \frac{tU_r^2}{v_f}, n' = \frac{nv_f}{U_r^2}, \theta = \frac{(T - T_\infty)}{(T_w - T_\infty)}$$

$$R = \frac{2\Omega v_f}{U_r^2}, M = \frac{B_0}{U_r} \sqrt{\frac{\sigma v_f}{\rho_f}}, \Pr = \frac{v_f}{\alpha_f}, S = \frac{w_0}{U_r}, K = \frac{kU_r^2}{v_f^2}, Q_H = \frac{Qv_r^2}{U_r^2 k_f}.$$
(2.14)

Using non-dimensional variables (2.14) the equations (2.2)–(2.4) yields the following dimensionless equations (dropping primes):

$$\left[1 - \phi + \phi \left(\frac{\rho_s}{\rho_f}\right)\right] \left(\frac{\partial u}{\partial t} - S\frac{\partial u}{\partial z} - Rv\right)
= \frac{1}{(1 - \phi)^{2.5}} \frac{\partial^2 u}{\partial z^2} + \left[1 - \phi + \phi \left(\frac{(\rho\beta)_s}{(\rho\beta)_f}\right)\right] \theta - \left(M^2 + \frac{1}{K}\right) u$$
(2.15)

$$\left[1 - \phi + \phi \left(\frac{\rho_s}{\rho_f}\right)\right] \left(\frac{\partial v}{\partial t} - S\frac{\partial v}{\partial z} + Ru\right) = \frac{1}{(1 - \phi)^{2.5}} \frac{\partial^2 v}{\partial z^2} - \left(M^2 + \frac{1}{K}\right) v, \tag{2.16}$$

$$\left[1 - \phi + \phi \left(\frac{(\rho C_p)_s}{(\rho C_p)_f}\right)\right] \left(\frac{\partial \theta}{\partial t} - S \frac{\partial \theta}{\partial z}\right) = \frac{1}{\Pr} \left(\frac{k_{nf}}{k_f} \frac{\partial^2 \theta}{\partial z^2} - Q_n \theta\right)$$
(2.17)

The velocity characteristic U_r is defined as (Hamad and Pop [24]).

$$U_r = \left[g\beta_f \left(T_w - T_\infty\right) v_f\right]^{\frac{1}{3}}.$$

Also the boundary conditions become

$$u = v = 0, \theta = 0, \text{ for } t \le 0$$
 (2.18)

$$u = 1 + \frac{\varepsilon}{2} \left\{ \exp(int) + \exp(-int) \right\}, \ v = 0, \ \theta'(0) = -\gamma \ (1 - \theta(0)) \ \text{at } z = 0$$

$$u \to 0, \ v \to 0, \ \theta \to 0 \ \text{as } z \to \infty$$

$$\begin{cases} v \to 0, \ \theta'(0) = -\gamma \ (1 - \theta(0)) \ \text{at } z = 0 \end{cases}$$

$$\begin{cases} v \to 0, \ \theta \to 0 \ \text{as } z \to \infty \end{cases}$$

Here $\gamma = \frac{h_f v_f}{K_f U_r}$ is the connective parameter. We now simplify (2.15) and (2.16) by putting the fluid velocity in the complex form as (let V = u + iv) to get

$$\left[1 - \phi + \phi \left(\frac{\rho_s}{\rho_f}\right)\right] \left(\frac{\partial V}{\partial t} - S\frac{\partial V}{\partial z} + iRV\right)
= \frac{1}{(1 - \phi)^{2.5}} \frac{\partial^2 V}{\partial z^2} + \left[1 - \phi + \phi \left(\frac{(\rho\beta)_s}{(\rho\beta)_f}\right) \theta - \left(M^2 + \frac{1}{K}\right)V\right]$$
(2.20)



The associated boundary conditions (2.18) and (2.19) are written as follows:

$$V = 0, \theta = 0 \text{ for } t \le 0 \tag{2.21}$$

$$V\left(0\right) = 1 + \frac{\varepsilon}{2} \left\{ \exp\left(int\right) + \exp\left(-int\right) \right\}, \ \theta'\left(0\right) = -\gamma \left[\left(1 - \theta\left(0\right)\right) \right]$$
 for $t > 0$. (2.22)

To find the analytical solutions of the system of partial differential equations (2.17), (2.20) in the neighborhood of the plate under the boundary conditions (2.21), (2.22), we express, V and θ as (Ganapathy [30]).

$$V\left(z,\ t\right) = V_0 + \frac{\varepsilon}{2} \left[\exp\left(int\right) \ V_1\left(z\right) + \exp\left(-int\right) \ V_2\left(z\right) \right] \tag{2.23}$$

$$\theta(z, t) = \theta_0 + \frac{\varepsilon}{2} \left[\exp(int) \theta_1(z) + \exp(-int) \theta_2(z) \right]$$
(2.24)

for $\varepsilon << 1$. Appeal to the above equations (2.23) and (2.24) into the equations (2.17) and (2.20) respectively and equating the harmonic and non-harmonic terms and neglecting the higher order terms of ε^2 , we obtain the following equations:

$$\frac{1}{(1-\phi)^{2.5}}V_0'' + S\left(1-\phi+\phi\left(\frac{\rho_s}{\rho_f}\right)\right)V_0' - \left[iR\left\{1-\phi+\phi\left(\frac{\rho_s}{\rho_f}\right)\right\} + M^2 + \frac{1}{K}\right]V_0 + \left[1-\phi+\phi\left(\frac{(\rho\beta)_s}{(\rho\beta)_f}\right)\right]\theta_0 = 0$$
(2.25)

$$\frac{1}{(1-\phi)^{2.5}}V_1'' + S\left(1-\phi+\phi\left(\frac{\rho_s}{\rho_f}\right)\right)V_1' - \left[i\left(R+n\right)\left\{1-\phi+\phi\left(\frac{\rho_s}{\rho_f}\right)\right\} + M^2 + \frac{1}{K}\right]V_1 + \left[1-\phi+\phi\left(\frac{(\rho\beta)_s}{(\rho\beta)_f}\right)\right]\theta_1 = 0$$
(2.26)

$$\frac{1}{(1-\phi)^{2.5}}V_{2}'' + S\left(1-\phi+\phi\left(\frac{\rho_{s}}{\rho_{f}}\right)\right)V_{2}' - \left[i\left(R-n\right)\left\{1-\phi+\phi\left(\frac{\rho_{s}}{\rho_{f}}\right)\right\} + M^{2} + \frac{1}{K}\right]V_{2} + \left[1-\phi+\phi\left(\frac{(\rho\beta)_{s}}{(\rho\beta)_{f}}\right)\right]\theta_{2} = 0$$
(2.27)

$$\frac{k_{nf}}{k_f}\theta_0'' + \Pr S \left[1 - \phi + \phi \left(\frac{(\rho C_p)_s}{(\rho C_p)_f} \right) \right] \theta_0' - Q_H \theta_0 = 0$$
(2.28)

$$\frac{k_{nf}}{k_f}\theta_1^{"} + \Pr S \left[1 - \phi + \phi \left(\frac{(\rho C_p)_s}{(\rho C_p)_f} \right) \right] \theta_1^{'} - \left[in \Pr \left\{ 1 - \phi + \phi \left(\frac{(\rho C_p)_s}{(\rho C_p)_f} \right) \right\} + Q_H \right] \theta_1 = 0 \quad (2.29)$$

$$\frac{k_{nf}}{k_{f}}\theta_{2}'' + \Pr S \left[1 - \phi + \phi \left(\frac{(\rho C_{p})_{s}}{(\rho C_{p})_{f}} \right) \right] \theta_{21}' - \left[in \Pr \left\{ 1 - \phi + \phi \left(\frac{(\rho C_{p})_{s}}{(\rho C_{p})_{f}} \right) \right\} - Q_{H} \right] \theta_{2} = 0 \quad (2.30)$$

where, the primes denote differentiation w.r.t. z.

The corresponding boundary conditions can be written as

$$V_0 = V_1 = V_2 = 1$$
, $\theta'_0 = -\gamma (1 - \theta_0)$, $\theta'_1 = \gamma \theta_1$, $\theta'_2 = \gamma \theta_2$ at $z = 0$ (2.31)

$$V_0 \to 0$$
, $V_1 \to 0$, $V_2 \to 0$, $\theta_0 \to 0$, $\theta_1 \to 0$, $\theta_2 \to 0$ at $z \to \infty$ (2.32)

Solving the equations (2.25) - (2.30) under the boundary conditions (2.31), (2.32) we obtain the velocity and temperature.

The skin-friction coefficient C_f and the local Nusselt number N_u which are defined as

$$C_f = \frac{(T_w)_{z=0}}{\rho_f U_t^2} = \frac{1}{(1-\phi)^{2.5}} V'(0)$$
(2.33)

$$Nu = \frac{x \left(\frac{\partial T}{\partial z}\right)_{z=0}}{T_w - T_\infty} = -\frac{k_{nf}}{k_f} Re_x \theta'(0)$$
 (2.34)



where $Re_x = \frac{U_r x}{v_f}$ is the local Reynolds number.

$$\frac{Nu}{Re_x} = -\frac{k_{nf}}{k_f}\theta'(0) \tag{2.35}$$

3 Results and discussion

The heat transfer characteristics with nanoparticles are discussed and the numerical computations are presented in Figs. 2-12 and in Tables 1 and 2. Fig. 2 illustrates the influence of the magnetic field parameter M on the velocity distribution for Cu–water and Al_2O_3 —water nanofluids. It is clear from the figures that the velocity distribution across the boundary layer reduces with an increase in the magnetic field parameter M. The Lorentz force has the tendency to slow down the motion of the fluid in the boundary layer.

For different values of the permeability parameter K, the velocity distribution on the porous wall is plotted in Fig. 3 for Cu-water and Al₂O₃-water. It is obvious that the increased values of K tend to increasing of the velocity on the porous wall and so enhance the momentum boundary layer thickness. The velocity reduces with increasing rotation parameter R. Increasing the rotation reduces the momentum boundary layer thickness (Fig. 4). The Fig. 5 denotes the velocity profile with the variation on heat source parameter Q_H . The magnitude of the velocity increases with increasing Q_H throughout the fluid region. Fig. 6 demonstrates the effect of the suction/injection parameter S on the fluid velocity for both the nano fluids. The velocity of the fluid across the boundary layer decreases by increasing the suction parameter S for both the nanofluids. Also we see that as S increases, the velocity still approaches the same asymptotic value for large values of z. Thus hydrodynamic boundary layer thickness decreases with the suction parameter S. Fig. 7 illustrates the variation of the velocity distribution for various values of the nanoparticle volume fraction parameter ϕ . It is seen from these figures that the velocity distribution across the boundary layer decreases with the increase of ϕ . The Fig. 8 represents the velocity distribution with the different values of convection parameter γ for Cu–water and Al₂O₃ – water. Increased values of γ tend to increasing of the velocity and so enhance the momentum boundary layer thickness. Fig. 9 displays the temperature profiles for various values of the heat generation parameter Q_H for both nanofluids with nanoparticles Cu and Al_2O_3 . The temperature in the boundary layer region decreases with the increase in the heat generation parameter Q_H and as a consequence the thermal boundary layer thickness decreases. Fig. 10 presents typical profile for the temperature distribution for various values of the convective parameter γ for both nanofluids with nanoparticles Cu and Al_2O_3 . The figures indicate that temperature in the fluid field decreases on increasing γ in the boundary layer region and is maximum at the surface of the plate for both nanoparticles. Thus, by escalating γ , thermal boundary layer thickness enhances. So, we can interpret that the rate of heat transfer decreases with increase in convective parameter γ . This phenomenon is more prominent in the presence of nanofluid particle volume fraction ϕ . Fig. 11 demonstrates that the variation of suction parameter S on temperature for both the nanofluids. The temperature reduces with increasing suction parameter S. On increasing the suction parameter S the thermal boundary layer thickness reduces throughout the fluid region. The influence of nanoparticle volume fraction parameter ϕ on the temperature is shown in Fig. 12 for Cu-water and Al₂O₃ - water. The temperature profile increases with the increase in nanoparticle volume fraction parameter ϕ . Thus the thermal boundary layer thickness increases and tends asymptotically to zero as the distance increases from the boundary. The variation of the skin friction coefficient C_f and the Nusselt number $\frac{Nu}{Re_x}$ with $M, K, R, \gamma, Q_H, S, \phi$ are shown in Table 1 and Table 2 respectively. Table 1 shows that the skin friction coefficient C_f decreases with increasing parameters K and Q_H whereas the skin friction coefficient increases with increasing M, R, S, γ, ϕ for both the nanofluids with nanoparticles Cu and Al₂O₃. Also the Nusselt number increases with the increase in the all parameters γ , Q_H , S, ϕ for both the nanofluids with nanoparticles Cu and Al₂O₃. The variation of Nusselt number is much more considerable for nanofluids. It is to be noted that highest heat transfer rate is obtained for Cu due to its higher thermal conductivity compared to Al₂O₃. These results are in good agreement with those reported by Hamad and Pop [24] as shown in the Table 3.



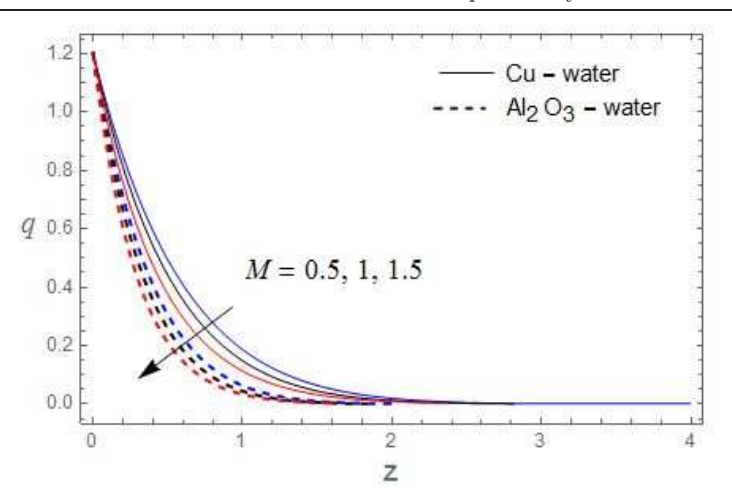


Fig. 2: The velocity profile for M with $K=0.5, R=0.5, \gamma=2, Q_H=1, S=1, \phi=0.05.$

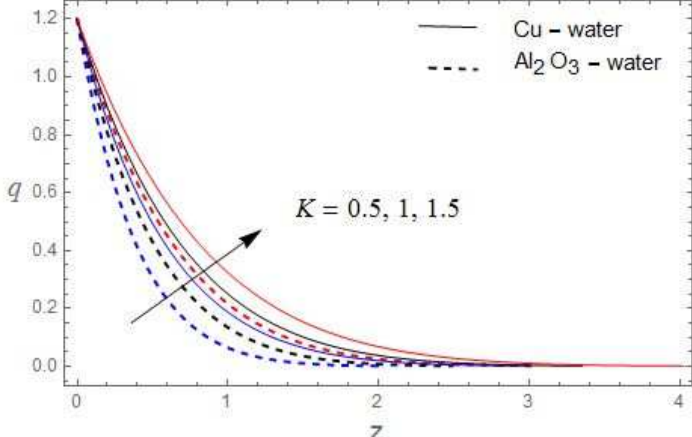


Fig. 3: The velocity profile for K with $M=0.5, R=0.5, \gamma=2, Q_H=1, S=1, \phi=0.05$.

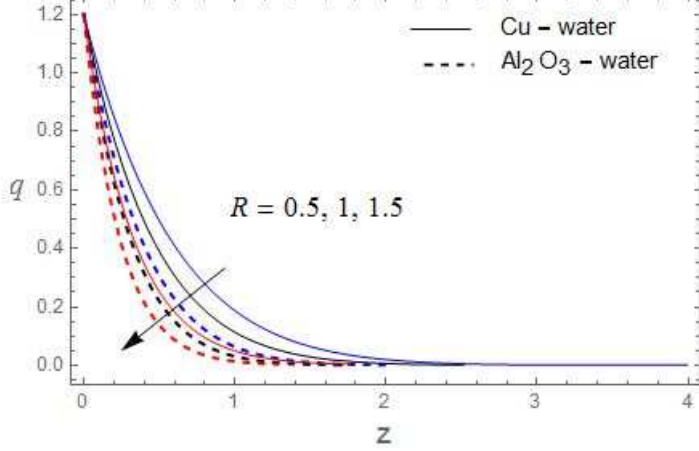


Fig. 4: The velocity profile for R with $M=0.5, K=0.5, \gamma=2, Q_H=1, S=1, \phi=0.05$.



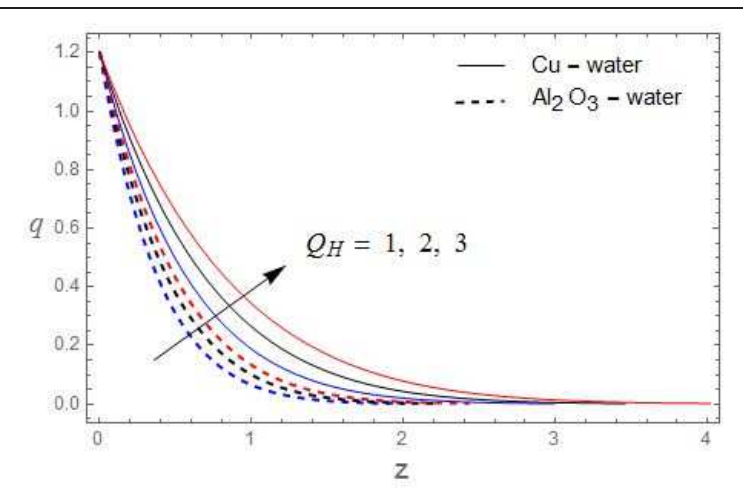


Fig. 5: The velocity profile for Q_H with $M=0.5, K=0.5, R=0.5, \gamma=2, S=1, \phi=0.05$.

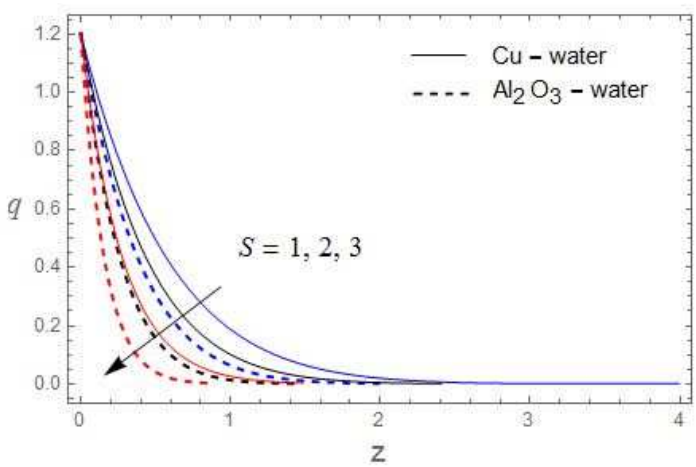


Fig. 6: The velocity profile for S with $M=0.5, K=0.5, R=0.5, \gamma=2, Q_H=1, \phi=0.05.$

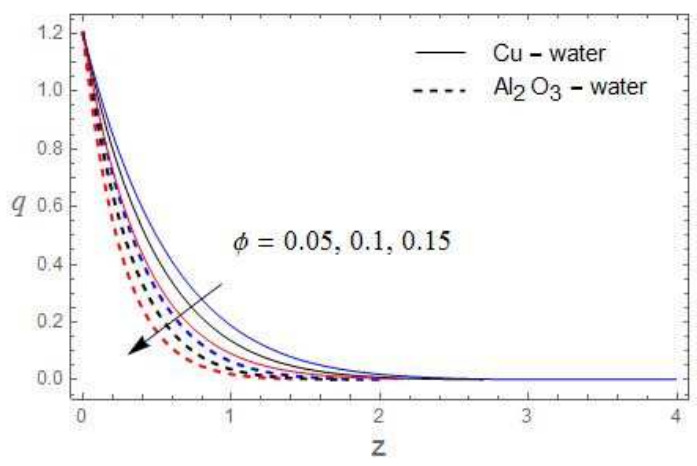


Fig. 7: The velocity profile for ϕ with $M=0.5, K=0.5, R=0.5, \gamma=2, Q_H=1, S=1.$



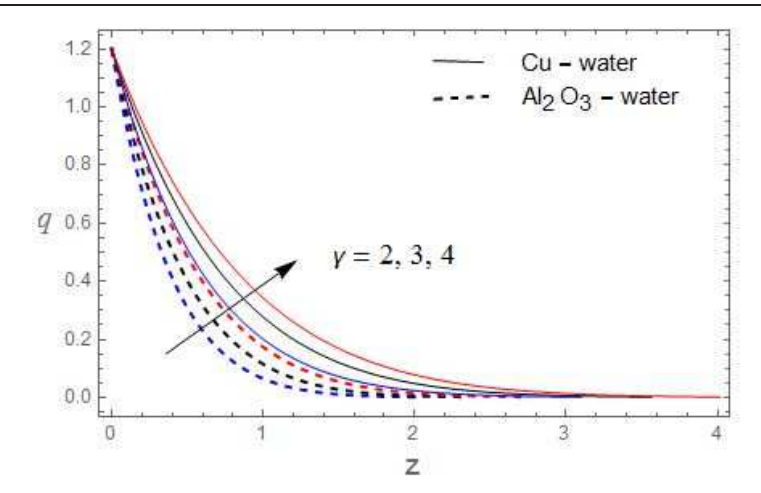


Fig. 8: The velocity profile for γ with $M=0.5, K=0.5, R=0.5, \phi=0.05, Q_H=1, S=1.$

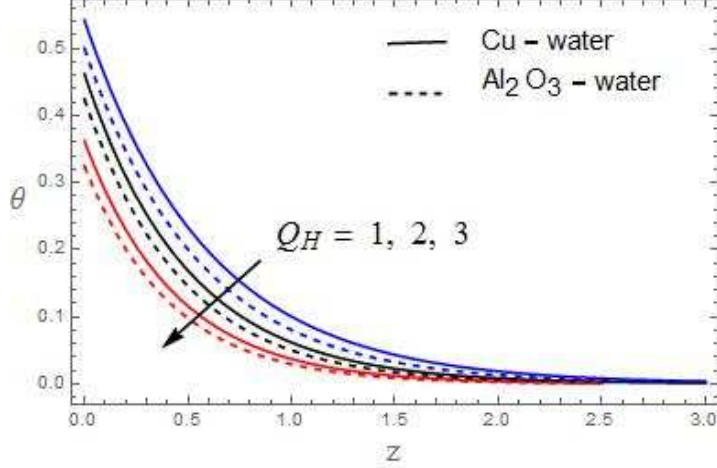


Fig. 9: The temperature profile for Q_H with $\gamma=2, S=1, \phi=0.05$.

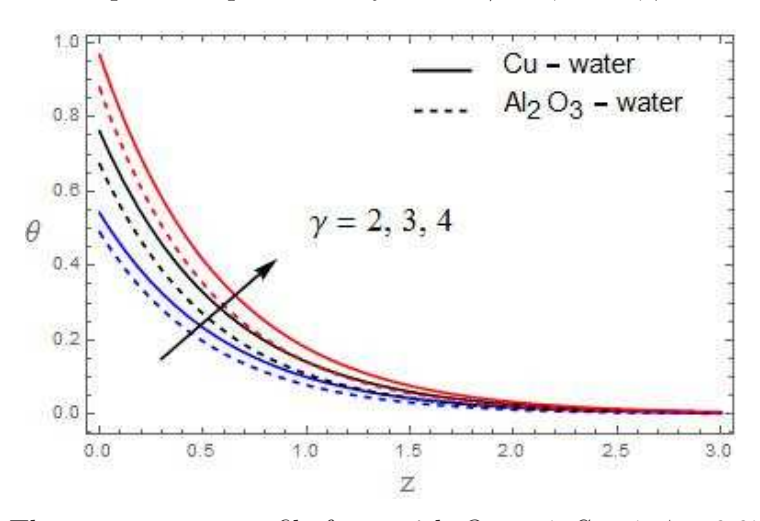


Fig. 10: The temperature profile for γ with $Q_H=1, S=1, \phi=0.05.$



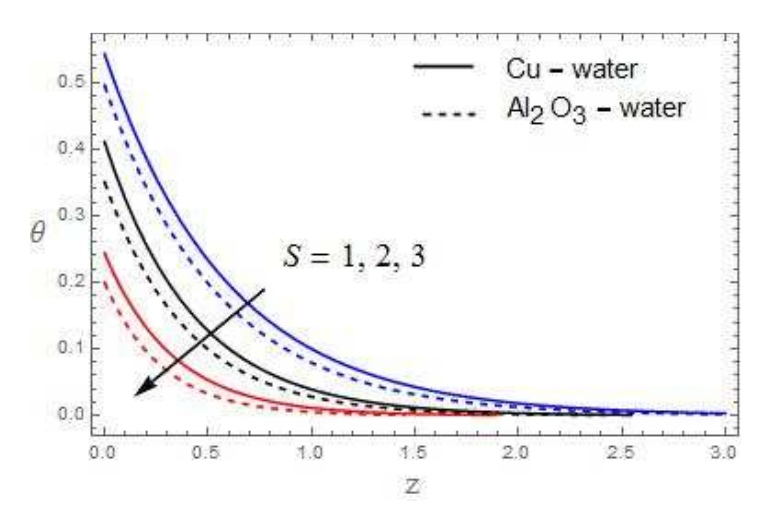


Fig. 11: The temperature profile for S with $\gamma=2, Q_H=1, \phi=0.05.$

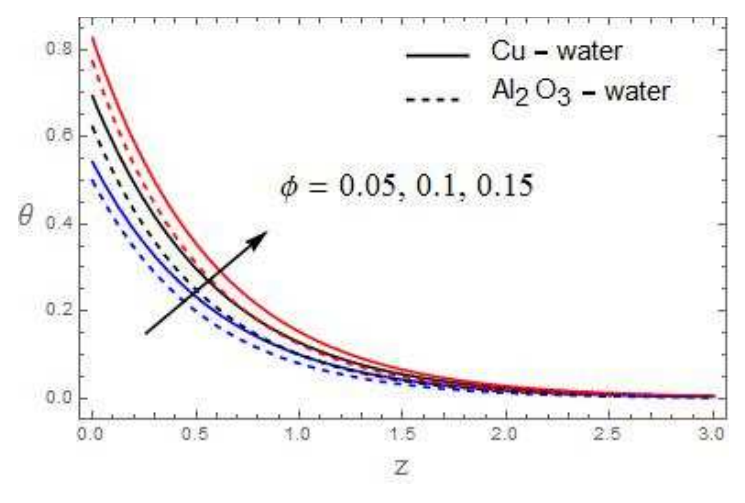


Fig. 12: The temperature profile for ϕ with $\gamma=2, Q_H=1, S=1.$



Table 1: Skin friction coefficient.

M	K	R	γ	Q_H	S	ϕ	C_f	C_f
							Cu-water	Al_2O_3 -
								water
0.5	0.5	0.5	2	1	1	0.05	2.64810	2.48975
1.0							2.85888	2.70528
1.5							3.17026	3.02161
	1.0						2.32620	2.15664
	1.5						2.20514	2.02935
		1.0					2.70750	2.53388
		1.5					2.79460	2.60039
			3				2.68215	2.52462
			4				2.70453	2.54712
				2			2.61773	2.45318
				3			2.59828	2.43068
					2		3.63795	3.25461
					3		4.80327	4.16210
						0.10	3.01702	2.68524
						0.15	3.41451	2.89714

Table 2: Local Nusselt number (Nu/Re_x) .

Q_H	γ	S	ϕ	Cu - water	Al_2O_3 - water
1	2	1	0.05	0.779717	0.733261
2				0.844371	0.808269
3				0.890440	0.860109
	3			0.927487	0.862487
	4			1.024570	0.945832
		2		0.983947	0.919390
		3		1.117110	1.051350
			0.10	0.844161	0.787435
			0.15	0.900935	0.780187

Table 3: Comparison of results for Local Nusselt number (Nu/Re_x) .

Q_H	S	ϕ	Cu – water results of	Cu– water results of
			Hamad and Pop [24].	the present study
				as $\gamma \to 0$.
1	1	0.05	0.688574	0.733261
2			0.744748	0.808269
3			0.856998	0.860109
	2		0.895578	0.919390
	3		1.002578	1.051350
		0.10	0.785549	0.787435
		0.15	0.884785	0.780187



4 Conclusions

The following conclusions are drawn from this study:

- 1. The fluid velocity decreases with the increase in the magnetic field parameter, the suction parameter, the nanoparticle volume fraction and the rotational parameter but this effect is reverse for the permeability parameter in the boundary layer region.
- 2. An increase in the convective parameter and nanoparticle volume fraction leads to an increase in the thermal boundary layer thickness but opposite effect occurs for the heat generation parameter.
- 3. The skin friction coefficient increases with the increase in the nanoparticle volume fraction, the magnetic field parameter, the suction parameter and the rotation parameter and it reduces with the permeability parameter.
- 4. The increasing values of Q_H , S, ϕ and γ is to increase the wall temperature gradient for both the nanofluids throughout the fluid region.

Acknowledgments The authors are grateful to the referees and the Editor-in-Chief for their helpful comments which have improved the quality of the paper.

References

- [1] Choi, S.U.S. (1995). Enhancing thermal conductivity of fluids with nanoparticles, *Devels. Appls. Non-Newtonian Flows*, 66, 99–105.
- [2] Masuda, H., Ebata, A., Teramea, K. and Hishinuma, N. (1993). Altering the thermal conductivity and viscosity of liquid by dispersing ultrafine particles, *Netsu Bussei*, 4(4), 227–233.
- [3] Eastman, J.A., Choi, S.L.S.S., Yu, W., Thompson, L.J. (2001). Anomalously increased effective thermal conductivity of ethylene glycol-based nanofluids containing copper nanoparticles, *Appl. Phys. Lett.*, 78(6), 718–720.
- [4] Xuan, Y. and Li, Q. (2003). Investigation on convective heat transfer and flow features of nanofluids, J. Heat Transf., 125, 151–155.
- [5] Minsta, H.A., Roy, G., Nguyen, C.T. and Doucet, D. (2009). New temperature dependent thermal conductivity data for water based nanofluids, *Int. J. Ther. Sci.*, 48, 363–371.
- [6] Buongiorno, J. and Hu, L.W. (2005). Nanofluid coolants for advanced nuclear power plants, Proceedings of ICAPP, Seoul, May 15–19, 260–272.
- [7] Kuznetsov, A.V. and Nield, D.A. (2010). Natural convective boundary layer flow of a nanofluid past a vertical plate, *Int. J. Ther. Sci.*, 49, 243–247.
- [8] Khan, W.A. and Aziz, A. (2011). Natural convection flow of a nanofluid over a vertical plate with uniform surface heat flux, *Int. J. Ther. Sci.*, 50, 1207–1214.
- [9] Kundu, P.K., Das, K. and Jana, S. (2014). Nanofluid flow towards a convectively heated stretching surface with heat source/sink: a lie group analysis, Afr. Mat., 25, 363-377. https://doi.org/10. 1007/s13370-012-0124-4
- [10] Das, K. (2012). Slip flow and convective heat transfer of nanofluids over a permeable stretching surface, *Comput. Fluids*, 64, 34–42.
- [11] Das, K. (2013). Lie group analysis for nanofluid flow past a convectively heated stretching surface, Appl. Math. Comput., 221, 547–557.
- [12] Das, K. (2014). Nanofluid flow over a shrinking sheet with surface slip, *Microfluid Nanofluid*, 16, 391–401.
- [13] Gilles, G.R., Nguyen, Cong Tam and Lajoie, Paul-René (2004). Numerical investigation of laminar flow and heat transfer in a radial flow cooling system with the use of nanofluids, Super Lattices Microstr., 35, 497–511.
- [14] Jou, R.Y. and Tzeng, S.C. (2006). Numerical research of nature convective heat transfer enhancement filled with nanofluids in rectangular enclosures, *Int. Commun. Heat Mass Transf.*, 33, 727–736.



- [15] Ho, C.J., Chen, M.W. and Li, Z.W. (2007). Effect of natural convection heat transfer of nanofluid in an enclosure due to uncertainties of viscosity and thermal conductivity, *Proceedings of ASME/JSME Thermal Engineering Summer Heat Transfer Conference-HT 1*, 833–841.
- [16] Ho, C.J., Chen, M.W. and Li, Z.W. (2008). Numerical simulation of natural convection of nanofluid in a square enclosure: effects due to uncertainties of viscosity and thermal conductivity, *Int. J. Heat Mass Transf.*, 51, 4506–4516.
- [17] Congedo, P.M., Collura, S. and Congedo, P.M. (2009). Modeling and analysis of natural convection heat transfer in nanofluids, *Proceedings of ASME Summer Heat Transfer Conference*, 3, 569–579.
- [18] Ghasemi, B. and Aminossadati, S.M. (2009). Natural convection heat transfer in an inclined enclosure filled with a water-CuO nanofluid, Num. Heat Transf. Part A Appl., 55, 807–823.
- [19] Khanafer, K., Vafai, K. and Lightstone, M. (2003). Buoyancy-driven heat transfer enhancement in a two dimensional enclosure utilizing nanofluids, Int. J. Heat Mass Transf., 46, 3639–3653.
- [20] Kim, J., Kang, Y.T. and Choi, C.K. (2004). Analysis of convective instability and heat transfer characteristics of nanofluids, *Phys. Fluids*, 16, 2395–2401.
- [21] Bakr, A.A. (2011). Effects of chemical reaction on MHD free convection and mass transfer flow of a micropolar fluid with oscillatory plate velocity and constant heat source in a rotating frame of reference, *Commun. Nonlinear Sci. Num. Simul.*, 16, 698–710.
- [22] Das, K. (2011). Effect of chemical reaction and thermal radiation on heat and mass transfer flow of MHD micropolar fluid in a rotating frame of reference, Int. J. Heat Mass Transfer, 54, 3505–3513.
- [23] Tiwari, R.K. and Das, M.K. (2007). Heat transfer augmentation in a two sided lid-driven differentially heated square cavity utilizing nanofluids, *Int. J. Heat Mass Transf.*, 50, 2002–2018.
- [24] Hamad, M.A.A. and Pop, I. (2011). Unsteady MHD free convection flow past a vertical permeable flat plate in a rotating frame of reference with constant heat source in a nanofluid, *Heat Mass Transf.*, 7, 1517–1524.
- [25] Aziz, A. (2009). A similarity solution for laminar thermal boundary layer over a flat plate with a convective surface boundary condition, *Commun. Nonlinear Sci. Num. Simul.*, 14, 1064–1068.
- [26] Makinde, O.D. and Aziz, A. (2010). MHD mixed convection from a vertical plate embedded in a porous medium with a convective boundary condition, Int. J. Ther. Sci., 49, 1813–1820.
- [27] Ishak, A. (2010). Similarity solutions for flow and heat transfer over a permeable surface with convective boundary condition, *Appl. Math Comput.*, 217, 837–842.
- [28] Yacob, N.A., Ishak, A., Pop, I. and Vajravelu, K. (2011). Boundary layer flow past a stretching/shrinking surface beneath an external uniform shear flow with a convective surface boundary condition in a nanofluid, *Nanoscale Res. Lett.*, 6, 314–319.
- [29] Liron, N. and Wilhelm, H.E. (1974). Integration of the magnetohydrodynamic boundary layer equations by Meksyn's method, *J. Comput. Appl. Maths (ZAMM)*, 54, 27–37.
- [30] Ganapathy, R. (1994). A note on oscillatory Couette flow in a rotating system, ASME J. Appl. Mechs. 61, 208–209.
- [31] Maxwell, J. (1904). A Treatise on Electricity and Magnetism, second ed., Oxford University Press, Cambridge, UK.
- [32] Brinkman, H.C. (1952). Viscosity of concentrated suspensions and solution, J. Chem. Phys., 20, 571–581.
- [33] Oztop, H.F. and Abu-Nada, v (2008). Numerical study of natural convection in partially heated rectangular enclosers with nanofluids, *Int. J. Heat Fluid Flow*, 29, 1326–1336.
- [34] Veera Krishna, M. and Chamkha, A.J. (2020). Hall and ion slip effects on MHD rotating boundary layer flow of nanofluid past an infinite vertical plate embedded in a porous medium, *Results in Physics*, 15, 102652. DOI: https://doi.org/10.1016/j.rinp.2019.102652
- [35] Veera Krishna, M. and Chamkha, A.J. (2019). Hall effects on MHD squeezing flow of a water based nano fluid between two parallel disks, *Journal of Porous Media*, 22(2), 209–223. DOI: https://doi.org/10.1615/JPorMedia.2018028721
- [36] Veera Krishna, M. and Chamkha, A.J. (2020). Hall and ion slip effects on unsteady MHD convective rotating flow of nanofluids application in Biomedical Engineering, *Journal of Egyptian Mathematical Society*, 28(1), 1–14. DOI: https://doi.org/10.1186/s42787-019-0065-2



Appendix

$$A_{1} = \frac{\gamma (1 - \phi)^{2.5} \left[1 - \phi + \phi \left(\frac{(\rho \beta)_{s}}{(\rho \beta)_{f}} \right) \right]}{(m_{1} + \gamma) (m_{1}^{2} - S_{1} m_{1} - B_{1})}, \tag{A.1}$$

$$m_1 = \frac{1}{2} \left[S_1 \operatorname{Pr}_1 + \sqrt{(S_1 \operatorname{Pr}_1)^2 + 4Q_H \frac{k_f}{k_{nf}}} \right],$$
 (A.2)

$$m_j = \frac{1}{2} \left[S_1 + \sqrt{(S_1)^2 + 4B_j - 1} \right], \quad j = 2, 3, 4,$$
 (A.3)

$$B_1 = M_1 + iR_1, (A.4)$$

$$B_2 = M_1 + i(R_1 + n_1), B_3 = M_1 + i(R_1 - n_1), \tag{A.5}$$

$$S_1 = S \left(1 - \phi \right)^{2.5} \left[1 - \phi + \phi \left(\frac{\rho_s}{\rho_f} \right) \right], \tag{A.6}$$

$$R_1 = R \left(1 - \phi \right)^{2.5} \left[1 - \phi + \phi \left(\frac{\rho_s}{\rho_f} \right) \right], \tag{A.7}$$

$$n_1 = n \left(1 - \phi\right)^{2.5} \left[1 - \phi + \phi \left(\frac{\rho_s}{\rho_f}\right)\right],\tag{A.8}$$

$$M_1 = \left(M^2 + \frac{1}{K}\right) (1 - \phi)^{2.5},$$
 (A.9)

$$\Pr_{1} = \frac{\Pr k_{f} \left[1 - \phi + \phi \left(\frac{\left(\rho C_{p} \right)_{s}}{\left(\rho C_{p} \right)_{f}} \right) \right]}{k_{nf} (1 - \phi)^{2.5} \left[1 - \phi + \phi \left(\frac{\rho_{s}}{\rho_{f}} \right) \right]}.$$
(A.10)

